

## Determination of Rutin in Pharmaceutical Formulations Using Admittance Biosensor Based on DNA and Nano Composite Film Using Coulometric FFT Admittance Voltammetry

P. Norouzi<sup>1,2,\*</sup>, B. Larijani<sup>3\*</sup>, M. R. Ganjali<sup>1,2</sup>, F. Faridbod<sup>1,2</sup>

<sup>1</sup>Center of Excellence in Electrochemistry, University of Tehran, Tehran, Iran

<sup>2</sup>Biosensor Research Center, Endocrinology and Metabolism Molecular-Cellular Sciences Institute, Tehran University of Medical Sciences, Tehran, Iran

<sup>3</sup>Endocrinology & Metabolism Research Center, Endocrinology and Metabolism Clinical Sciences Institute, Tehran University of Medical Sciences, Tehran, Iran

\*E-mail: [norouzi@khayam.ut.ac.ir](mailto:norouzi@khayam.ut.ac.ir); [emrc@tums.ac.ir](mailto:emrc@tums.ac.ir)

Received: 30 May 2013 / Accepted: 27 September 2013 / Published: 23 March 2014

---

A novel Rutin FFT admittance biosensor was fabricated based on ZrO<sub>2</sub> nanoparticles (NPs), graphene, ionic liquid, 1-butyl-3-methylimidazolium hexafluorophosphate (BMIMPF<sub>6</sub>) and DNA on glassy carbon electrode (GCE). The developed electrochemical method for determination of Rutin was based on coulometric fast Fourier transformation admittance voltammetry (CFFTAV). The admittance of Rutin increased significantly at DNA-ZrO<sub>2</sub> NPs/GRs-BMIMPF<sub>6</sub>/GCE compare to the bare GCE, GCE, indicating that the modification increases sensitivity of the detection process. The influence of important parameters in the determination process were investigated, and the experimental conditions were optimized. Also, for reaching to maximum sensitivity, Rutin effectively accumulated on the surface of the biosensor. The reduction admittance of the biosensor shows linearly in concentrations ranges of Rutin from 2 to 150 × 10<sup>-9</sup> M with a detection limit of 2.3 × 10<sup>-10</sup> M. Moreover, the proposed biosensor exhibited high sensitivity, fast response time (less than 7 s) and long-term stability. The proposed method was successfully used to the determination of Rutin content in the pharmaceutical formulation.

---

**Keywords:** FFT Coulometric Admittance Voltammetry; biosensor, Rutin, ZrO<sub>2</sub> nanoparticles, Graphene nanosheet

### 1. INTRODUCTION

Rutin (3', 4', 5, 7-tetrahydroxyflurone-3β-d-Rutinoside) is the most abundant bioactive flavonoid also called as vitamin P. Its schematic chemical structure of Rutin is shown in Fig. 1. Rutin

as a natural flavone derivative has a wide range of physiological activities including hemostat, anti-inflammatory, anti-tumor antibacterial and anti-oxidant [1-3].

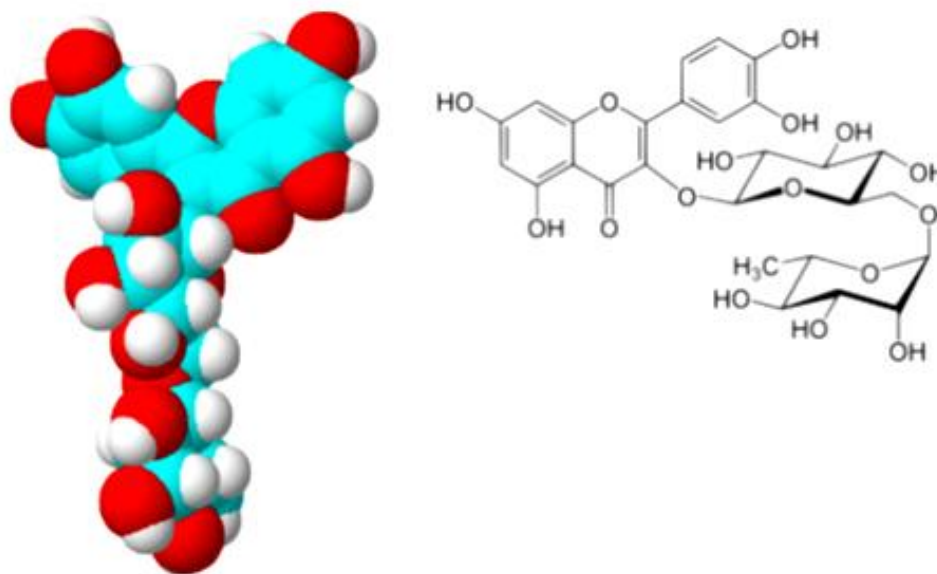


**Figure 1.** 3D and cChemical structure of the Rutin molecule

Metal oxide nanoparticles such as  $\text{CeO}_2$ ,  $\text{ZnO}$ ,  $\text{SnO}_2$ ,  $\text{TiO}_2$  and  $\text{ZrO}_2$  have recently been used for fabrication of enzyme-based biosensors [4-9].  $\text{ZrO}_2$  is considered as an ideal candidate of oxide for immobilization of biomolecules with oxygen groups. For example, DNA was immobilized on  $\text{ZrO}_2$  gel casting on glassy carbon electrode, and the resulting DNA-modified electrode was characterized with the cyclic voltammetry [10]. Also, Zhu et al. presented a simple and practical DNA hybridization detection based on  $\text{ZrO}_2$  thin films modified gold electrode for literature [11].

Graphene as a carbon nanomaterial exhibits high surface area and excellent electrical conductivity and it helps to introduce a larger number of active sites [12]. From this it is clear that the high conductivity can facilitate the electron transfer of electroactive species. Ionic liquids (IL) have individually been known to improve the electrocatalytic activity. In fact, IL was also used as an electrode modified material in our work due to its high ionic conductivity, good stability and well biocompatibility [13-17].

Rutin was analyzed previously by different electrochemical methods which will be discussed later. This work introduces a new electrochemical method for determination of Rutin based on coulometric FFT admittance voltammetry (CFFTAV) [18-23]. Using fast Fourier transformation algorithm for numerical electrochemical data provides a real time analysis. In modern electrochemistry, FFT has been used for digital signal processing and filtering. Since the bandwidth of the input signal is limited by an analog low pass filter ahead of the Analog to digital (A/D) converter, after collecting data in the computer memory, they are used for calculating the signal in the frequency domain.

Also, a new designed biosensor was fabricated by graphene nanosheets (GNS) which is mixed with 1-butyl-3-methylimidazolium hexafluorophosphate (BMIMPF<sub>6</sub>), and then ZrO<sub>2</sub> nanoparticles. The presence of GNs in DNA-ZrO<sub>2</sub>/GNS-BMIMPF<sub>6</sub>/GCE provides an environment, t which enhances the analyte response. Therefore, by using a more sensitive detection method and nano-composite film on the electrode, a more sensitive biosensor can be provided.

Scanning electron microscopy and impedance spectroscopy was used to characterize the proposed sensor. Under optimal conditions, the designed sensor exhibited a linear response to Rutin concentrations.

## 2. MATERIALS AND METHODS

### 2.1. Reagents

All chemicals and solvents used were of analytical grade and used as received. Double distilled water was used throughout the experiments. Rutin was purchased from Merck Co., The Rutin and was stored in the frozen state, and its standard solutions were prepared daily with double distilled water when in use. The prepared solutions were kept at 4 °C before use. Zirconium Oxide nanoparticles (ZrO<sub>2</sub> NPs, 99.0%, 20nm) were purchased from Nanostructured & Amorphous Materials, Inc. Graphene nanosheets (GNs) purchased from Sinopharm Henan Bonzer Co. Calf thymus DNA (ct-DNA) was purchased from Sigma. 1-butyl-3-methylimidazolium hexafluorophosphate (BMIM PF<sub>6</sub>) (>99%) was obtained from Merck Co. Solution of DNA was freshly prepared in 5 mM Tris-HCl buffer solution pH=7.5 (THB).

### 2.2. Biosensor Preparation

A glassy carbon electrode (GCE, 3 mm in diameter) were polished well with 1.0, 0.3 and 0.05 μm alumina slurry and then it was washed thoroughly with doubly distilled water. The electrodes were successively sonicated in 1:1 nitric acid, acetone and doubly distilled water, and then allowed to dry at room temperature.

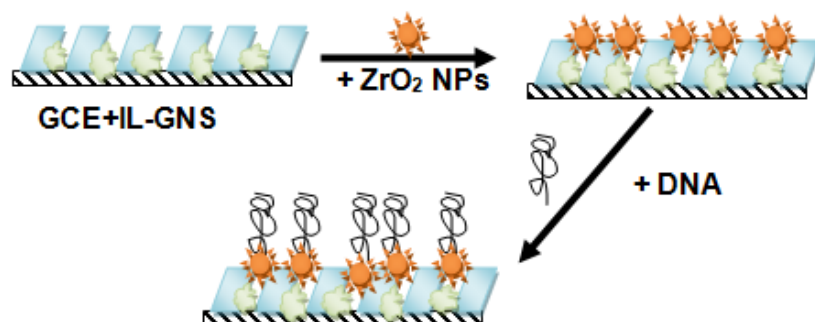


**Figure 2.** Schematic figures of DNA-ZrO<sub>2</sub>/GNS-BMIMPF<sub>6</sub>/GCE preparation

The fabrication of DNA-ZrO<sub>2</sub>/GNS-BMIMPF<sub>6</sub>/GCE biosensor involves three sequential stages. First, 10 mg of purified GNS were dispersed in 10 mL of dimethyl formamide (DMF) with the aid of ultrasonication for 2 h to give a 1.0 mg/mL homogeneous suspension. After that, BMIMPF<sub>6</sub> (final concentration (v/v) 3.0%) was dispersed in the GNS suspension with the aid of ultrasonication. 10 μL of the GNS-BMIMPF<sub>6</sub> suspension was dropped on the GCE and let it dry at room temperature for 3 h, thus a uniform membrane coated GNS-BMIMPF<sub>6</sub>/GCE was obtained. Finally, 6 micro-liters of ZrO<sub>2</sub>NPs (4 % (w/w) in DMF) was coated on GNS-BMIMPF<sub>6</sub>/GCE electrode dried in air to form the ZrO<sub>2</sub>/GNS-BMIMPF<sub>6</sub>/GCE, and then the electrode was immersed in a 2.5 mg/mL DNA solution, prepared freshly for adsorbing DNA, the resulting biosensor was denoted DNA-ZrO<sub>2</sub>/GNS-BMIMPF<sub>6</sub>/GCE, before the electrochemical experiments the electrode was rinsed with doubly distilled water for the removal of unabsorbed DNA.

### 2.3. Instrumentation

The electrochemical measurement system used, for admittance voltammetric measurements, was a homemade potentiostat [18-23], which was connected to a PC equipped with an analog to digital data acquisition board (PCL-818H, Advantech Co.). In the measurements, the memory and CPU requirements of the computer were dictated by the condition of the data acquisition requirements electrochemical software was developed using Delphi 6.0. The program was used to generate an analog waveform and acquire admittance readings. The potential waveform was repeatedly applied to the working electrode and then the data was acquired, and stored by the software. Also, in the program able to process and plot the data in real time, EIS measurements were performed in 3 mM K<sub>3</sub>Fe(CN)<sub>6</sub> in PBS at pH 7.5.

## 3. RESULTS AND DISCUSSION

In the beginning of the work, the electrochemical biosensor was fabricated using GNS-BMIMPF<sub>6</sub> composite film as matrix for to enhances the immobilized capacity toward DNA of the base electrode, which was favor to electron communication between the Rutin and the surface of the biosensor. Nanometer-sized ZrO<sub>2</sub>, GNS and BMIMPF<sub>6</sub> could accelerate the electron transfer between Rutin molecule and the electrode surface. ILs due to their interesting properties have recently found various applications in construction of electrochemical sensors and biosensors in order to modify the responses. Among the most important characteristics of ionic liquids, ionic conductivity, the width of the electrochemical potential window, viscosity, hydrophobicity and non-volatility cause the use of these solvents in electrochemical devices.

The DNA is attached to ZrO<sub>2</sub> and this provides a environment for the immobilization of various biomolecules and promotes electron transfer between the molecule and the electrode surface [24].

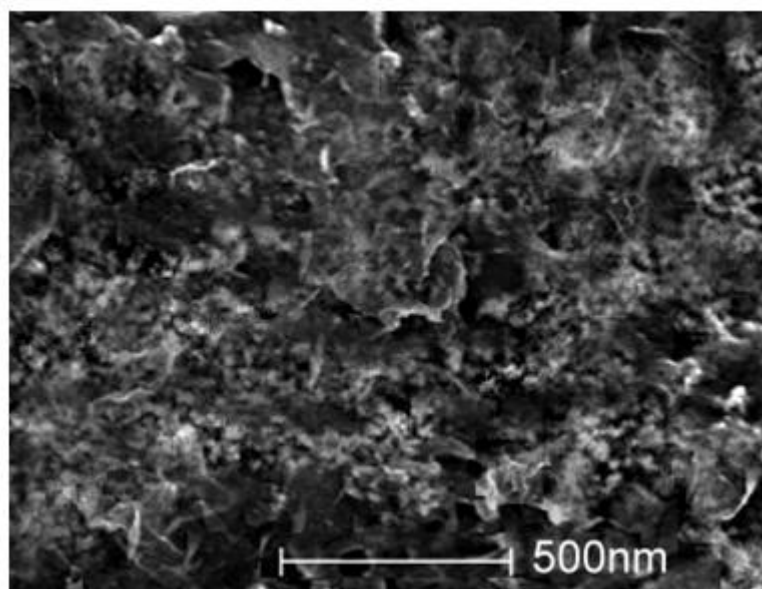


**Figure 3.** SEM images DNA-ZrO<sub>2</sub>/GNS-BMIMPF<sub>6</sub>/GCE biosensor.

Therefore, it is necessary the biosensor to be characterized. The surface morphologies of DNA-ZrO<sub>2</sub>/GNS-BMIMPF<sub>6</sub>/GCE composite was examined by SEM observation. Fig. 3 shows SEM image of DNA-ZrO<sub>2</sub>/GNS-BMIMPF<sub>6</sub>/GCE. The image clearly showed that a layer of compact ZrO<sub>2</sub> NPs was formed on the GNS-BMIMPF<sub>6</sub> surface, and ZrO<sub>2</sub> NPs were compactly embedded on the substrate. Also, it was worth notice that, the as-prepared GNS-BMIMPF<sub>6</sub> composite exhibited considerable edge plane structures. The GNS-BMIMPF<sub>6</sub> has lateral dimensions from a few hundred nanometers to several micrometers, and a thickness of 40 nm.

The results obtained using admittance voltammetry measurements are in agreement with the results obtained from EIS. Fig. 4A shows results of electrochemical impedance spectroscopic (EIS) measurements carried out on DNA-ZrO<sub>2</sub>/GNS-BMIMPF<sub>6</sub>/GCE biosensor GNS-BMIMPF<sub>6</sub>/GCE and GCE electrode in the buffer solution containing 3 mM [Fe(CN)<sub>6</sub>]<sup>3-/4-</sup>. It is assumed for the Randles circuit, the resistance to electron transfer and the diffusion impedance is parallel to the interfacial double layer capacitance. In this figure, the semicircle portion, observed at higher frequencies, corresponds to electron-transfer-limited process, whereas the linear part is characteristic of the lower frequencies range and represents the diffusion-limited electron-transfer process. It can be seen that semicircle diameter of DNA-ZrO<sub>2</sub>/GNS-BMIMPF<sub>6</sub>/GCE is larger than that of GCE, indicating higher electron transfer resistance at the electrode interface. The edge planes that were shown in SEM image have revealed to be essentially responsible for the higher electron transfer kinetics and the electrocatalytic activity of graphene. This can contribute significantly to the electrochemical property of the present DNA as well.

Fig. 4B showed the cyclic voltammograms of Rutin on GCE (curve a) and DNA-ZrO<sub>2</sub>/GNS-BMIMPF<sub>6</sub>/GCE (curve b) 0.05 M phosphate buffer solution at pH 7.5. The cyclic voltammetric studies for DNA-ZrO<sub>2</sub>/GNS-BMIMPF<sub>6</sub>/GCE biosensor in the buffer solution containing 3 mM [Fe(CN)<sub>6</sub>]<sup>3-/4-</sup> shows a well-defined peak with increased value of the peak current, which is very weak for the GC electrode.

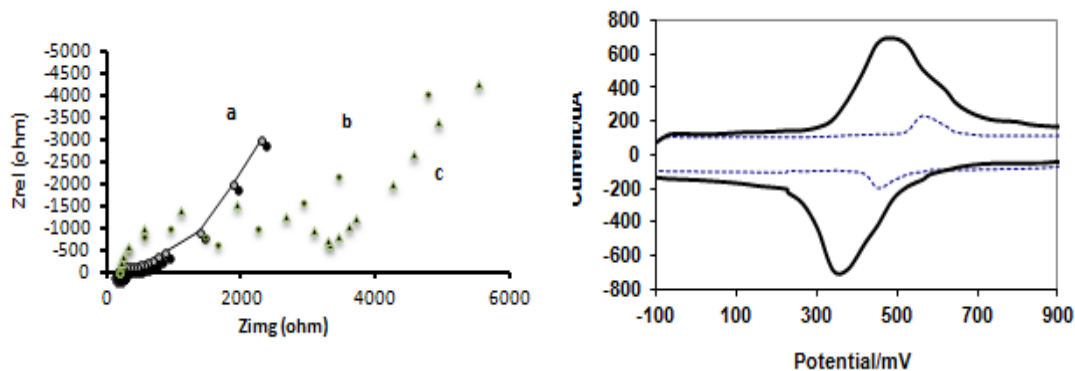


**Figure 4.** Cyclic voltammograms of 5 μM Rutin in buffer on (a) the bare GCE, and (b) DNA-ZrO<sub>2</sub>/GNS-BMIMPF<sub>6</sub>/GCE; scan rate 800 mV/s EIS plots of modified electrode in 3 mM K<sub>3</sub>Fe(CN)<sub>6</sub> with: (a) bare GCE (b) GNS-BMIMPF<sub>6</sub>/GCE and (c) DNA-ZrO<sub>2</sub>/GNS-BMIMPF<sub>6</sub>/GCE

Consequently, under such condition the active sites expose for its easier access to the substrate leading to improved coulometric response of the biosensor. Also, Rutin shows very weak redox peaks, at the bare GCE, this is an indication of the lower rate kinetic reaction of Rutin on the GCE surface.

On the other hand, for DNA-ZrO<sub>2</sub>/GNS-BMIMPF<sub>6</sub>/GCE shows well-defined redox peaks on the modified electrode, in which anodic and cathodic peak potentials were at about 380 mV and 490 mV, respectively, and the ratio of  $i_{pa}/i_{pc}$  was about 1.15, which showed that the electrode reaction was almost reversible. DNA-ZrO<sub>2</sub>/GNS-BMIMPF<sub>6</sub>/GCE can enhance the electron-transfer rate and make more Rutin participate in the electrochemical reaction due to their accumulation and catalytic ability.

### 3.1. Determination method

It is well known that many fundamental microscopic processes take place at the electrode surface, which can lead to the overall electrical signals. For determination of Rutin, the current passing through the biosensor was sampled during the potential ramp and the admittance of the biosensor was calculated. Then, coulometric signal was calculated by integrating of net admittance changes is applied over the selected scanned potential range. The biosensor response (charge change under the peak) was calculated as;

$$\Delta Q = Q - Q_0 \tag{1}$$

where Q is the electrical charge obtained by integration of admittance voltammetric curve between 0 and 700 mV, and Q<sub>0</sub> represents Q in the absence of the adsorbent. In this method, ΔQ is calculated based on the -admittance changes at the voltammograms in the integration potential range of the admittance. Moreover, the results indicate that with increasing the concentration of Rutin in the injected sample, ΔQ increases proportionally.

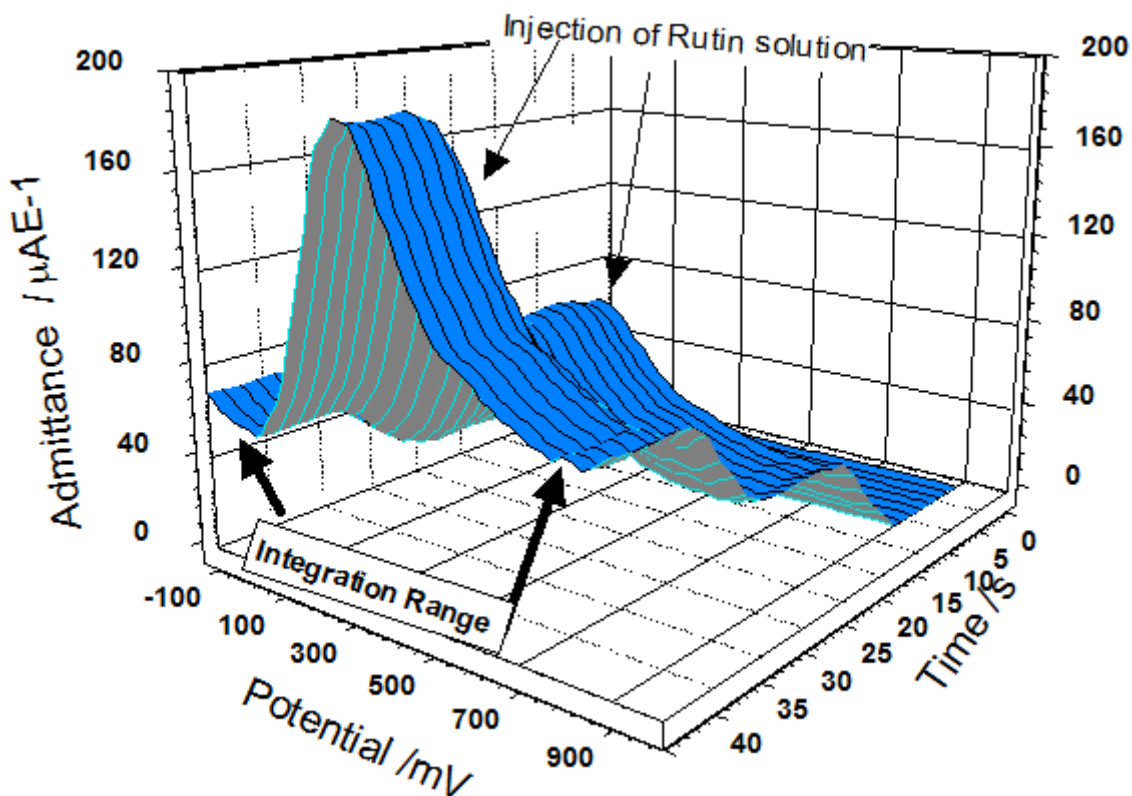


**Figure 5.a)** FFT admittance voltammograms of the DNA-ZrO<sub>2</sub>/GNS-BMIMPF<sub>6</sub>/GCE biosensor in absent and with addition of  $3.0 \times 10^{-6}$  M Rutin in the buffer solution at pH 7.5; The potential range of -100 to 900 mV at frequency 550 Hz and amplitude 20 mV. Integration potential range for the admittance is 100 to 800 mV.

Fig. 5 shows CFETA and the changes in voltammetric response of the DNA-ZrO<sub>2</sub>/GNS-BMIMPF<sub>6</sub>/GCE biosensor in the potential range of -100 to 900 mV. The potential axis on this graph represents potential applied to the working electrode during each potential scan. The time axis represents the time passing between the beginning of the experiment and the beginning of a particular sweep (i.e. it represents a quantity proportional to the sweep number) [2425-2728]. The figure shows that after addition of  $33.0 \times 10^{-6}$  M Rutin in the buffer solution at pH 7.5 a signal appears at potential 370 mV. The integration range for the admittance is in range of -100 to 800 mV. The increase in the admittance at potential 370 mV can be due to the redox of Rutin at electrode surface. However, as mentioned above the accumulation of Rutin on the high surface area of DNA-ZrO<sub>2</sub>/GNS-BMIMPF<sub>6</sub>/GCE can enhance of direct electron transfer between the active sites of the biosensor. This can increase the peak admittance at the recorded voltammograms, when the sample was added to the solution.

### 3.2. Optimization of SW frequency and amplitude

It is well known that the admittance coulometric voltammetric response of the analyte depends on the applied SW frequency and amplitude.

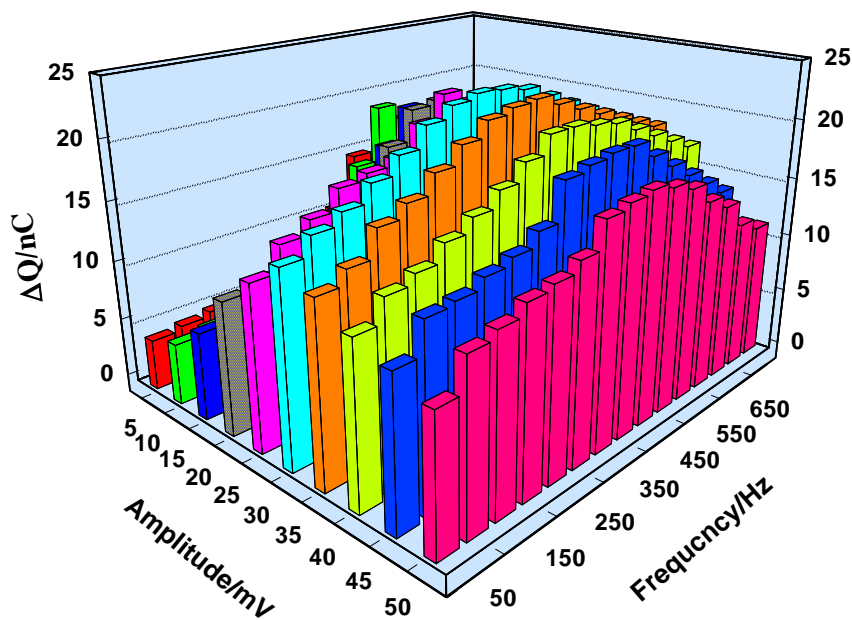


**Figure 6.** The effect of frequency and amplitude on the response of DNA-ZrO<sub>2</sub>/GNS-BMIMPF<sub>6</sub>/GCE to additions of 2.0 × 10<sup>-6</sup> M Rutin, the potential range of -100 to 900 mV. Integration potential range for the admittance is 100 to 800 mV

To obtain the optimum SW wave form condition in for maximum  $\Delta Q$ , the SW frequency range 50-700 Hz and amplitude 5 to 50 mV were studied. In Fig. 6 the importance of frequency and amplitude is demonstrated for solution of 2  $\mu$ M of Rutin. Since the signal, background noise, and peak shape of Rutin, depends on condition of excitation signal. Therefore, the solution resistance, electrode diameter, and stray capacitance of the system will limit the sensitivity gains obtained by raising the SW frequency. It can be say that SW frequency and amplitude can play similar roles as sweep rate in cyclic voltammetry. As it can be seen that increasing the SW frequency and amplitude will increase the admittance of the DNA-ZrO<sub>2</sub>/GNS-BMIMPF<sub>6</sub>/GCE biosensor, may due to enhancement in value of the electron transfer. The figure shows enhancement frequency up to 550 Hz and amplitude up to 20 mV themV the value of  $\Delta Q$  increase, and after that a decline in the response can be observed. Therefore application of very high SW frequencies causes a shorter potential scan times.

It can be suggested that at the higher values of frequency and amplitude due to short time for the electrochemical process on the electrode surface. Consequently, the response becomes smaller. Application SW frequencies lower than 550 Hz causes a longer potential scan times, which result to lower number of voltammetric scan ( as well as the data points of  $\Delta Q$ ) for each injected sample zone.

### 3.2. Optimization of pH

The dependence of the DNA-ZrO<sub>2</sub>/GNS-BMIMPF<sub>6</sub>/GCE response to Rutin solution in various pH values was investigated. Fig. 7 shows the result of examination of pH on the biosensor sensitivity. The following measurements were recorded at frequency 550 Hz and amplitude 20 mV. The



reversibility of reaction was more clearly shown in acidic medium. If the pH was increasing oxidation admittance was decreasing and oxidation potential was less positive. Also, it was seen that the redox peak potential shifted to the negative direction with the increase of buffer pH, indicating that protons took part in the electrode reaction.

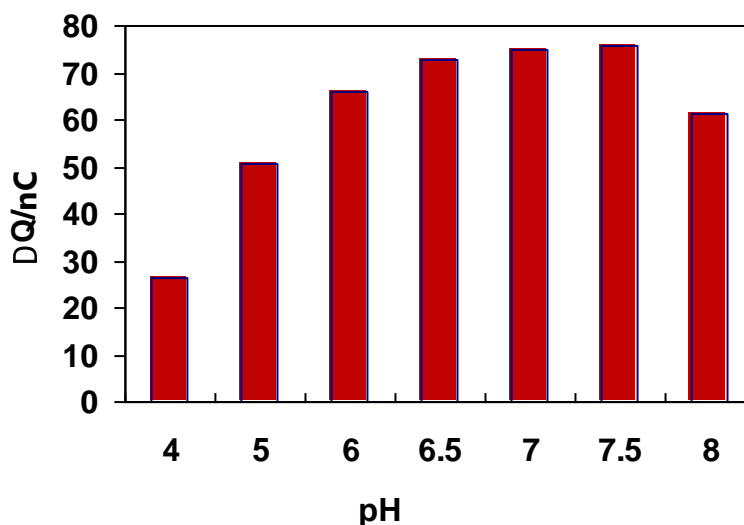


**Figure 7.** The effect of pH concentration on biosensor response to additions of  $5.0 \times 10^{-6}$  M Rutin, the potential range of -100 to 900 mV at frequency 550 Hz and amplitude 20 mV. Integration potential range for the admittance is 100 to 800 mV

The result shows showed that the slope value of  $-55.3$  mV/pH was close to theoretical value of  $-59$  mV/pH, demonstrating that the ratio of electron and proton taking part in the electrode reaction was 1:1. The maximum value of reduction peak current response appeared at the pH value of 7.5 and decreased gradually with the further increase increment of the buffer pH. The results indicated that proton involved in the electrochemical reaction at the mild basic solution. Therefore, pH 7.5 was selected as the optimal pH for detection in the following experiments.

#### 3.4. Calibration curve and biosensor characterization

As mentioned above the electrode response could be expressed in various ways as  $\Delta Q$  (in  $\mu\text{C}$ Coulomb). For this reason, the magnitude of the addition peaks depends on the choice of the integration range.

#### 3.5. Analytical procedures

A stock solution of 5 mM Rutin was firstly prepared, and then an aliquot was diluted to the appropriate concentration. Before each FFTCAV measurement, the three-electrode system was installed in a blank solution, and then standard solutions weresolutions were added,and the admittance voltammetry scan from  $-100$  to  $900$  mV vs. SCE.

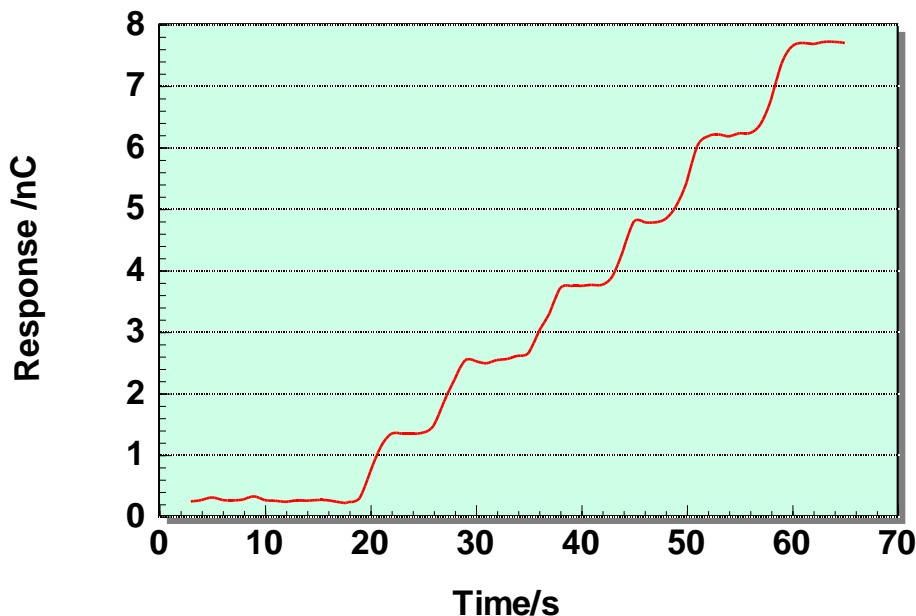


**Figure 8.** Response of the DNA-ZrO<sub>2</sub>/GNS-BMIMPF<sub>6</sub>/GCE to upon the following concentrations: a, 100 to 600 nM of Rutin solutions. The potential range of -100 to 900 mV at frequency 550 Hz and amplitude 20 mV; Integration potential range for the admittance is 100 to 800 mV

Fig. 8 illustrates a typical  $\Delta Q$  response of the DNA-ZrO<sub>2</sub>/GNS-BMIMPF<sub>6</sub>/GCE on a standard solution of Rutin (from 100 to 600 nM in PB solution, at pH7.5), where the experimental parameters were set at optimum values in order to obtain the best detection limits for the biosensor.

Results shown in this figure represent the integrated signal for 3 consecutive additions of the Rutin standard solution. Under optimized conditions, the steady-state voltammetry showed a linear dynamic range of 2 to 120 nM (Fig. 9).

A correlation coefficient of  $R=0.997$  with %R.S.D. values 2.9%. All measurements carried out for small analyte concentrations allow the estimation of the detection limit and the linearity was evaluated by linear regression analysis. The detection limit, estimated based on signal to noise ratio ( $S/N=3$ ), was found to be  $0.23 \pm 0.02$  nM.

### 3.5. Analytical procedures

The method was used to determine Rutin in pharmaceutical tablets. The typical sample preparation was as follows: five tablets were weighed accurately and ground finely with a pestle and a mortar. The precise amount of powder was dissolved in ethanol absolute, sonicated and centrifuged. The clear solution was filtered, diluted and stored at 4 °C in a refrigerator. Prior to measurement, the stock solution was further diluted with the buffer solution.

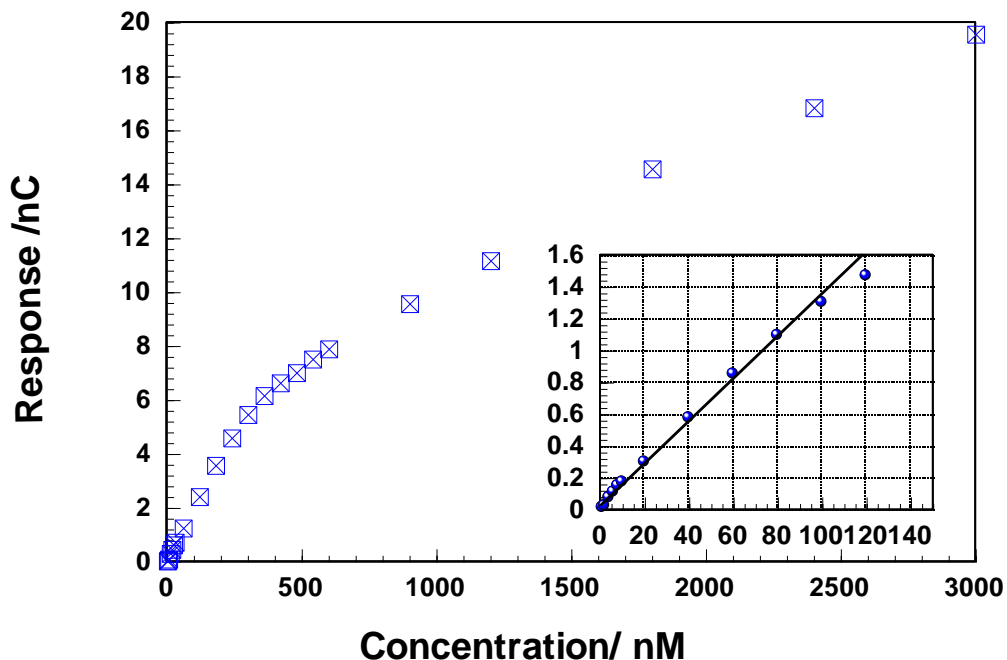


**Figure 9.** The calibration curve for Rutin standard solutions in pH 7.5; The the potential range of -100 to 900 mV at frequency 550 Hz and amplitude 20 mV; Integration potential range for the admittance is 100 to 800 mV

Standard addition method was applied to determine Rutin content at DNA-ZrO<sub>2</sub>/GNS-BMIMPF<sub>6</sub>/GCE biosensor. In these measurements, the obtained recoveries for the spike samples were ranged from 98.9% to 102.6% and the contents of Rutin found are in good agreement with that specified by the manufacturers (20 mg/tablet). The results are shown in Table 1.

These results indicate that the proposed voltammetry method has acceptable precession and accuracy for rapid and sensitive determination of Rutin in pharmaceutical tablets.

Also, in evaluation, the performances of the fabricated biosensor is compared with some of the best previously reported Rutin sensors based on the utilization of different materials as the working electrode and different detection techniques (Table 2) and it was confirmed that the presented DNA-ZnO<sub>2</sub>Nps ZrO<sub>2</sub>Nps and GNS-BMIMPF<sub>6</sub> based Rutin biosensor with CFFTA V exhibited an excellent and reproducible sensitivity [2829–3233].

**Table 1.** Determination of Rutin in pharmaceutical tablets by standard addition method (concentration in (nM)

Samples	Detected	Added	Found	Recovery (%)
1	6.2	6.0	12.2	99.5
2	10.5	20.0	30.9	101.3
3	43.5	40.0	82.5	99.3
4	43.9	40.0	83.9	101.1

**Table 2.** The comparison of the proposed biosensor with the best previous reported ones based on the utilization of different materials

Ref.	Detection Method	DL	Materials
2829	Voltammetry	$1.0 \times 10^{-8}$ M	IL/CPE
2930	Voltammetry	$1.5 \times 10^{-8}$ M	MCM-41/CPE
3031	Voltammetry	$3.2 \times 10^{-8}$ M	AuNPs/en/MWNTs/GCE
3132	Square-wave voltammetric	$2.0 \times 10^{-8}$ M	Gilo/Chi/epichlorohydrin/GCE
3233	Reversing differential pulse voltammetry	$4.0 \times 10^{-8}$ M	MCNTPE
This work	CFFTAV	$2.3 \times 10^{-10}$ M	DNA-ZrO <sub>2</sub> /GNS-BMIMPF <sub>6</sub> /GCE

Using FFT function for filtering the noises causes an improvement in S/N ratio. Besides, using new composite of graphene nanosheets, ZrO<sub>2</sub> NPs and ionic in construction of biosensor causes a better conversion of the chemical signal to electrical ones. Since the proposed biosensor can determine lower amount of Rutin rather than other methods.

Using fast Fourier transform (FFT) method was found very helpful mathematical method in combination by designed potential waveform to repeatedly apply to the working electrode for trace analysis. The approach is designed to process the voltammetric signal and calculate the biosensor admittance by using discrete FFT method. Also, in this way, some of the noises are digitally filtrated and decrease the bandwidth of the measurement. Further improvement in the signal of the analyte was gained by admittance integration of the biosensor response in a selected potential range of the voltammogram.

### 3.6. Stability and reproducibility of the Biosensor

The biosensor was evaluated by examining the analyte response, using CFFTAV method. The long-term storage stability of the DNA-ZrO<sub>2</sub>/GNS-BMIMPF<sub>6</sub>/GCE biosensor was tested for 60 days electrode at room temperature when not in use. The sensitivity retained  $92.5 \pm 0.2\%$  of initial sensitivity up to 60 days which gradually decreases afterwards might be due to the loss of the catalytic activity.

## 4. CONCLUSIONS

In this work, a highly sensitive Rutin electrochemical method accompanied with a new biosensor has been developed for determination of Rutin. DNA-ZrO<sub>2</sub>/GNS-BMIMPF<sub>6</sub>/GCE was fabricated by modifying the GC electrode surface. A higher producible sensitivity of  $3.4 \mu\text{CnM}/\text{cm}^{-2}$ , response time less than about 7 s, and detection limit of  $0.23 \pm 0.02 \text{ nM}$ , was observed. Under optimal

conditions, the designed sensor exhibited a wide linear response to Rutin concentration, good sensitivity, a fast response time, repeatability (R.S.D value of 2.9%) and long term stability, However, application other mathematical methods in signal processing seem to be promising in increasing the method sensitivity.

#### ACKNOWLEDGEMENT

The authors are grateful to the Research Council of University of Tehran for the financial support of this work.

#### References

1. R.M. Gene, C. Cartana, T. Adzet, E. Marin, T. Panella, and S. Canigueral, *Planta Med.*, 62 (1996) 232
2. A. Hasan, I. Ahmad, *Fetoterapia*, 67 (1996) 182
3. R. Ramanathan, W.P. Das, C.H. Tan, *Int. J. Oncol.*, 3 (1993) 115
4. S.T. Jiang, Z. P. Chen, Q. Z. Diao, S. C. Sheng, G. M. Xie, M. J. Zhang, and H. J. Xu, *Acta Chim. Sinica* 70 92012) 2085
5. P. Nayak, B. Anbarasan, and S. Ramaprabhu, *J. Phys. Chem. C* 117 (2013) 13202
6. A. K. Yang, Y. Xue, Y. Zhang, X. F. Zhang, H. Zhao, X. J. Li, Y. J. He, and Z. B. Yuan, *J. Mater. Chem. B* 1 (2013) 1804
7. F. Bentiss, M. Lebrini, N. E. Chihib, M. Abdalah, C. Jama, M. Lagrenée, S. S. Al-Deyab and B. Hammouti, *Int. J. Electrochem. Sci.*, 7 (2012) 3939
8. A. A. Ensafi, H. Bahrami, B. Rezaei, and H. Karimi-Maleh, *Mater. Sci. Eng. C* 33 (2013) 831
9. S. Reddy, S. B. E. Kumara, and H. Jayadevappa, *Electrochim. Acta* 61 (2012) 78
10. E. Boisselier, D. Astruc, *Chem. Soc. Rev.*, 38 (2009) 1759
11. J. Perez-Juste, I. Pastoriza-Santos, L.M. Liz-Marzan, P. Mulvaney, *Coord. Chem. Rev.*, 249 (2005), pp. 1870
12. N.N. Zhu, A.P. Zhang, Q.J. Wang, P.G. He, and Y.Z. Fang, *Anal. Chim. Acta*, 510 (2004) 163
13. F. Faridbod, M. R. Ganjali, M. Pirali-Hamedani and P. Norouzi, *Int. J. Electrochem. Sci.*, 5 (2010) 1103
14. M. R. Ganjali, H. Khoshsafar, A. Shirzadmehr, M. Javanbakht and F. Faridbod, *Int. J. Electrochem. Sci.*, 4 (2009) 435
15. P. Norouzi, H. Rashedi, T. Mirzaei Garakani, R. Mirshafian and M. R. Ganjali, *Int. J. Electrochem. Sci.*, 5 (2010) 377
16. M. Zhang, A. Smith, and W. Gorski, *Anal. Chem.*, 76 (2004) 5045
17. G.C. Zhao, M.Q. Xu, J. Ma, X.W. Wei, *Electrochem. Commun.*, 9 (2007), 920.
18. P. Norouzi, M. R. Ganjali, B. Larijani, A. Mirabi-Semnokolaii, F. S. Mirnaghi, and A. Mohammadi, *Pharmazie* 63 (2008) 633.
19. P. Norouzi, M. R. Ganjali, S. Shirvani-Arani, and A. Mohammadi, *J. Pharm. Sci.* 95 (2007) 893.
20. M. R. Pourjavid, P. Norouzi, and M. R. Ganjali, *Int. J. Electrochem. Sci.* 4 (2009) 923.
21. P. Norouzi, G. R. NabiBidhendi, M. R. Ganjali, A. Sepehri, M. Ghorbani, *Microchimica Acta*, 152 (2005) 123.
22. P. Norouzi, M. R. Ganjali, T. Alizadeh, and P. Daneshgar, *Electroanalysis*, 18 (2006) 947.
23. P. Norouzi, M. R. Ganjali, A. Sepehri, and M. Ghorbani, *Sens. Actuators B* 110 (2005) 239.
24. Z. Tong, R. Yuan, Y. Chai, S. Chen, Y. Xie, *Biotechnol Lett.* 29 (2007) 791.
25. P. Norouzi, B. Larijani, M. Ezoddin and M. R. Ganjali, *Mater. Sci. Eng. C* 28(2008)87.

26. M. R. Ganjali, P. Norouzi, R. Dinarvand, R. Farrokhi, and A. A. Moosavi-Movahedi, *Mater. Sci. Eng. C* 28 (2008) 1311.
27. P. Norouzi, M. R. Ganjali, and L. Hajiaghababaei, *Anal. Lett.*, 39 (2006) 1941.
28. M. R. Ganjali, P. Norouzi, M. Ghorbani, and A. Sepehri, *Talanta*, 66 (2005) 1225.
29. Y. Zhang, J.B. Zheng, *Talanta* 77 (2008) 325.
30. X.F. Xie, D.Z. Zhou, X.J. Zheng, W.S. Huang, K.B. Wu, *Anal. Lett.* 42 (2009) 678.
31. S. Yang, L. Qu, G. Li, R. Yang, C. Liu, *J. Electroanal. Chem.* 645 (2010) 115.
32. I.R.W.Z. de Oliveira, S.C. Fernandes, I.C. Vieira, *J. Pharm. Biomed. Anal.* 41 (2006) 366.
33. X.Q. Lin, J.B. He, Z.G. Zha, *Sens. Actuat. B* 119 (2006) 608.

© 2014 The Authors. Published by ESG ([www.electrochemsci.org](http://www.electrochemsci.org)). This article is an open access article distributed under the terms and conditions of the Creative Commons Attribution license (<http://creativecommons.org/licenses/by/4.0/>).